

# Chapter 7

## EXPERIMENTAL RESULTS FOR COMPACTED SAND

This chapter reports the experimental results regarding effects of an adjacent inclined rock face on earth pressure at-rest for compacted sand. Fig. 7.1 shows the rock face inclination angle considered are  $\alpha = 0^\circ, 45^\circ, 60^\circ, 70^\circ$  and  $80^\circ$ . The height of backfill behind the non-yielding wall is 1.5 m. To obtain the expected dense condition, the loose backfill was compacted with two different soil vibratory compactors. The compacted dense sand has relative density  $D_r = 72\%$ , and a unit weight  $\gamma = 16.5 \text{ kN/m}^3$ . Based on direct shear tests (Ho, 1999), the corresponding internal friction angle  $\phi$  for the dense backfill is  $40.1^\circ$ . The testing program is listed in Table 7.1.

### 7.1 Distribution of lateral earth pressure at $\alpha = 0^\circ$

The distribution of lateral earth pressure for the dense backfill compacted with 2 different compactors at  $\alpha = 0^\circ$  (no steel interface plate) is discussed in this section. Test results are compared with Jaky (1944), Peck and Mesri (1987), and Chen (2002).

#### 7.1.1 Backfill Compacted with a Square Compactor

The distributions of lateral earth pressure against the non-yielding wall, after the backfill was compacted in five 0.3 m-thick lifts with the square compactor (Fig. 3.7)

are shown in Fig. 7.2 (a) to Fig. 7.2 (e). The variation of lateral earth pressure was monitored by soil pressure transducer mounted on the model wall. Before compaction, the earth pressure at-rest can be properly estimated with Jaky's equation. After compaction, Fig. 7.2 (d) shows that an extra horizontal stress  $\Delta\sigma_{h,ci}$  was induced by compaction. From Fig. 7.2 (d), it is clear that the compaction-influence zone. The compaction-influenced zone extended from the compacted surface to the depth of approximately 0.7 m. Peck and Mesri (1987) indicated that the compaction induced lateral pressure near the surface is limited by the passive earth pressure with Rankine's theory. The lateral earth pressure near the base of the wall is related to the overburden and can be estimated with Jaky's equation. In Fig. 7.2 (e), the lateral stress measured near the top of backfill is almost identical to passive earth pressure. In Fig. 7.2 (c) to (e), the lateral stresses measured below the compaction-influenced zone converge to the earth pressure at-rest based on Jaky's equation.



### 7.1.2 Backfill Compacted with Strip Compactor

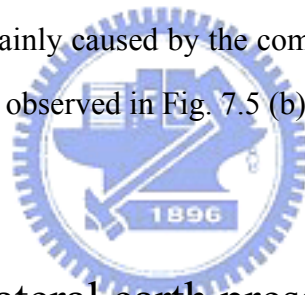
Fig. 7.3 shows the distributions of lateral earth pressure for the dense backfill compacted with the strip vibratory compactor (Fig. 3.9). The 1.5 m-thick backfill was compacted in fifteen 0.1 m-thick lifts. The relative density of soil obtained is 72 %. The lateral stress distribution for  $\alpha = 0^\circ$  are shown in Fig. 7.3 (a) to (e). The compaction-influenced zone extended from the compacted surface to the depth of approximately 1.1 m.

### 7.1.3 Comparison of Test Results

Fig. 7.4 shows the distribution of lateral stress for backfills densified with two compactors for  $\alpha = 0^\circ$ . It is found that the lateral earth pressure induced by the strip compactor is higher than that induced by the square compactor. It should be mention that, to achieve the relative density of 72 %. The backfill was divided into 15 lifts (Fig. 5.7), and each lift is compacted into 15 lanes (Fig. 5.9) by the strip compactor. The

amount of energy input for the strip compactor is about 7.5 times as much as that for the square compactor.

The stress path ( $\sigma_v$  versus  $\sigma_h$ ) for a soil element under compaction by strip compactor is shown in Fig. 7.5. Chen (2002) indicated that the compaction process will not result in any residual stress in the vertical direction. On the other hand, horizontal earth pressure increases significantly due to compaction. The test data shown in Fig. 7.5(a), (b), and (c). were measured by SPT02, SPT05, and SPT12 respectively. The path F represents the stress variation due to the filling of the 0.1 m-thick. Stress path C represents the stress variation due to compaction on top of surface. From these figures, It is clear that at SPT02, compaction causes the  $\sigma_h$  to increase on stress path C2, C3 and C4. The Rankine earth pressure is the upper bound of the induced pressure. The  $\sigma_h$  decreases with the compaction of the 5<sup>th</sup> lift C5. Variation of lateral stress is mainly caused by the compaction process, not soil filling. Similar stress variation can be observed in Fig. 7.5 (b) and (c)



## 7.2 Distribution of lateral earth pressure at various $\alpha$

### Angles

The distribution of lateral earth pressure regarding sand compacted with 2 different compactors are discussed in this section. Fig. 7.6 (a) shows the distribution of lateral earth pressure against the non-yielding wall at interface inclination angle  $\alpha = 45^\circ$  (Fig. 4.10). The backfill was compacted in five 0.3 m-thick lifts. In Fig. 7.6 (a), the measured earth pressure is clearly affected by rough interface inclined at  $\alpha = 45^\circ$ . The measured stress is lower than Jaky's solution at the elevation 0.9 m to 0. An extra horizontal stress  $\Delta\sigma_{h,ci}$  was induced by compaction at the elevation from 1.5 m to 0.9 m. The compaction-influenced zone extended from the compacted surface to the depth of approximately 0.6 m. The compaction induced lateral pressure near the

surface is limited by the Rankine passive pressure as suggested by Peck and Mesri (1987). The lateral stress increased slowly with the increasing depth from the elevation 0.9 m to 0.25 m. However, the measured lateral pressure decreased with depth from the elevation 0.25 m to 0.

Fig. 7.6 (b) shows the distribution of lateral stress for the fill compacted with the strip compactor at  $\alpha = 45^\circ$ . The backfill was compacted in fifteen 0.1 m-thick lifts. The measured stress is lower than Jaky's solution from the elevation 0.8 m to 0. An extra horizontal stress  $\Delta\sigma_{h,ci}$  was induced by compaction at elevation 1.5 m to 0.8 m. The compaction-influenced zone extended from the compacted surface to the depth of approximately 0.7 m and the compaction induced lateral pressure near the surface is also limited by the Rankine passive pressure. However, the measured lateral pressure decreased with depth from the elevation 0.8 m to 0. In Fig. 4.10, the interface plate is located closer to the soil pressure transducers for the lower part of the model wall. As a result, the  $\sigma_h$  measured would be affected by the approaching of the interface plate.

Fig. 7.7 (a) shows the distribution of lateral earth pressure for  $\alpha = 60^\circ$  with square compactor. The measured stress is lower than Jaky's solution at elevation 0.9m to 0 especially near the base of wall. It may be observed in Fig. 4.11(a), with the increase of  $\alpha$  angle, the distance between the model wall and the interface plate decreased. The compaction-influenced zone extended from the compacted surface to the depth of approximately 0.6 m and the lateral stress near the surface is limited by passive earth pressure.

Fig. 7.7 through 7.9 show the distribution of earth pressure for a compacted fill with the interface inclination  $\alpha = 60^\circ, 70^\circ,$  and  $80^\circ$ . It may be observed in these figures that the compaction induced stresses near the surface is limited by the Rankine passive pressure. At the lower part of the wall, the  $\sigma_h$  decreases with the approaching of the inclined rock face.

Fig. 7.10 shows the distribution of lateral earth pressure for the dense backfill compacted with square compactor with the rock face inclination angle  $\alpha = 0^\circ, 45^\circ,$  and  $60^\circ$ . In this Figure, the lateral earth pressures measured for  $\alpha = 45^\circ$  and  $60^\circ$  are lower

than Jaky's solution from the elevation 0.9 m to 0. The magnitude of  $\sigma_h$  decreased with the increase of  $\alpha$  angle at 0.9 m to 0.25 m and decreased slowly with depth from the elevation 0.25 m to 0. The compaction-influenced zone extended from the compacted surface to the depth of approximately 0.6 m. However, the maximum  $\Delta\sigma_{h,ci}$  decreased with increasing  $\alpha$  angle approximately at the elevation of 1.15 m. The compaction induced lateral stress near the surface is limited by Rankine passive pressure.

Fig. 7.11 shows the distribution of lateral stress for the dense backfill compacted with the strip compactor. In this Figure, below the compaction-influenced zone, the measured lateral stresses for  $\alpha = 45^\circ, 60^\circ, 70^\circ,$  and  $80^\circ$  are lower than Jaky's solution. For  $\alpha = 70^\circ$  and  $80^\circ$ , the distribution of lateral stress is similar to that for  $\alpha = 60^\circ$ . The depth of compaction-influenced zone decreased with increasing interface inclination angle  $\alpha$ . This phenomenon may be explained with the help of Fig. 5.9. For  $\alpha = 0^\circ$ , compaction was compacted from Lane 1 through Lane 15 for the top layer. However, for  $\alpha = 80^\circ$ , compaction was carried out only from Lane 13 to Lane 15 for the top layer. The effective compaction depth is significantly influenced by the amount of energy input.

## 7.3 At-Rest Soil Thrust

### 7.3.1 Magnitude of At-Rest Soil Thrust

The variation of horizontal at-rest pressure coefficient  $K_{o,h}$  as a function of interface inclination angle is shown in Fig. 7.12. The coefficient  $K_{o,h}$  for loose sand are compared with that for the backfill compacted with 2 different compactors. It is seen that, with the same interface inclination angle, the order of coefficient is  $K_{o,h,strip} > K_{o,h,square} > K_{o,h,loose}$ . In Fig. 7.12, the coefficient  $K_{o,h}$  for backfill compacted with square compactor, the coefficient  $K_{o,h}$  decreases with increasing rock

face inclination angle  $\alpha$ . The coefficient  $K_{o,h}$  for sand compacted with the strip compactor is approximately 0.67 at  $\alpha = 0^\circ$ . Due to the compaction effect coefficient, the  $K_{o,h}$  is clearly higher than Jaky's prediction. However, with the increase of the rock face inclination, the coefficient  $K_{o,h}$  decreases.

Fig. 7.13 shows the horizontal lamina of Ottawa sand. The lamina of Ottawa sand was between the lower part of the model wall and inclined interface plate. Janssen (1895) and Reimbrt and Reimbert (1954) reported the silo equation to estimate the distribution of the horizontal pressure with stored material. The coefficient of friction between stored material and wall was considered. The lateral stress decreases with increasing coefficient of friction. Spangler and Handy (1984) indicated granular backfill placed in the relatively narrow gap between the wall and the natural rock face is partly supported by friction on each side, from the wall and from the rock face. Since the friction is distributed vertically it reduces vertical stress within the soil mass, which in turn reduces the horizontal stress and the overturning moment. In this study, the horizontal lamina of Ottawa sand was narrow between the lower part of the model wall and the inclined interface plate for  $\alpha = 70^\circ$  and  $80^\circ$ . The inclined interface plate closes to SPT extremely so that the vertical earth pressure is affected by friction between the inclined interface plate and Ottawa sand. The vertical stress was decreased by friction. The horizontal stress  $\sigma_h$  decreases with decreasing vertical stress relatively.

### 7.3.2 Point of Application of At-Rest Soil Thrust

The point of application  $h/H$  of the total thrust as a function of the rock face inclination angle  $\alpha$  is discussed in this section. Fig. 7.14 shows, without the interface plate ( $\alpha = 0^\circ$ ), due to the compaction induced stress near the top of the wall, the point of application of the at-rest soil thrust for compacted sand is located at about 0.49 H to 0.50 H above the base of the wall. As the interface angle  $\alpha$  increases, the earth pressure near the base of the wall (Fig. 7.11) start to decrease. This change of

earth pressure distribution causes the total thrust to rise to higher locations as shown in Fig.7.14. For  $\alpha = 80^\circ$ , the point of application of the total thrust for backfill compacted with strip compactor is located at  $0.68 H$  above the base of the wall. Due to the compacted effect, at the same inclination angle  $\alpha$ , the order of  $h/H$  for compacted and loose sand is  $(h/H)_{\text{strip}} > (h/H)_{\text{square}} > (h/H)_{\text{loose}}$ .

Fig. 7.15 shows the overturning moments above the base,  $M_o$  at various  $\alpha$ . From this figure, the driving moments are less than Jaky's solution. The overturning moments  $M_o$  decreased with increasing inclination angle of rock face  $\alpha$ .  $M_o$  is clearly affected by friction of inclined interface plate and Ottawa sand.

